

## Article

# Experimental Study of Surface Roughness of Pine Wood by High-Speed Milling

Chunmei Yang <sup>1,2</sup>, Yaqiang Ma <sup>1,2</sup>, Tongbin Liu <sup>1,2</sup>, Yucheng Ding <sup>2,3,\*</sup> and Wen Qu <sup>1,2,\*</sup>

<sup>1</sup> College of Mechanical and Electrical Engineering, Northeast Forestry University, Harbin 150040, China; ycmnefu@nefu.edu.cn (C.Y.); myqhit@nefu.edu.cn (Y.M.); ltb1161879674@nefu.edu.cn (T.L.)

<sup>2</sup> Forestry and Woodworking Machinery Engineering Technology Center, Northeast Forestry University, Harbin 150040, China

<sup>3</sup> College of Computer and Control Engineering, Northeast Forestry University, Harbin 150040, China

\* Correspondence: dingyucheng@nefu.edu.cn (Y.D.); qwen@nefu.edu.cn (W.Q.)

**Abstract:** The surface roughness of wood has a great influence on its performance and is a very important indicator in processing and manufacturing. In this paper, we use the central composite design experiment (CCD experiment) and artificial neural network (ANN) model to study the changing pattern of surface roughness during the high-speed milling process of pine wood. In the CCD experiments, the spindle speed, feed speed, and depth of cut are used as the influencing factors, and the surface roughness is used as the index to analyze the variation law and fit the surface roughness parameter equation. By measuring the chip size in each group in the CCD experiment, the ANN model is used to predict the surface roughness under this machining parameter by measuring the chip size in each test group. The experimental results showed that the mean error of the surface roughness prediction values in the CCD experiment (12.2%) was larger than that of the ANN model (7.8%), and the mean squared error (MSE) of the ANN model was 0.025, the mean absolute percentage error (MAPE) was 0.01, and the coefficient of determination  $R^2$  was 0.95. Compared with the CCD experiment, the ANN model had a higher prediction accuracy. The results of this paper can provide some guidance for the prediction of surface roughness during wood processing.

**Keywords:** surface roughness; pine wood; CCD experiment; ANN model; chips size



**Citation:** Yang, C.; Ma, Y.; Liu, T.; Ding, Y.; Qu, W. Experimental Study of Surface Roughness of Pine Wood by High-Speed Milling. *Forests* **2023**, *14*, 1275. <https://doi.org/10.3390/f14061275>

Academic Editor: Byung-Dae Park

Received: 7 May 2023

Revised: 4 June 2023

Accepted: 14 June 2023

Published: 20 June 2023



**Copyright:** © 2023 by the authors. Licensee MDPI, Basel, Switzerland. This article is an open access article distributed under the terms and conditions of the Creative Commons Attribution (CC BY) license (<https://creativecommons.org/licenses/by/4.0/>).

## 1. Introduction

Wood is one of the most predominant biomass composites, which has received a lot of attention from the research community due to its renewable nature and innovative applications [1,2]. In wood products, the surface quality of wood has a significant effect on gluing and painting [3], and the basic criterion for surface quality is the surface roughness of wood, and the quality of wood products depends to a large extent on the surface roughness [4]. Studies have shown that the bonding properties and painting of wood products are significantly improved when the surface quality of the wood is higher, i.e., when the surface roughness is smaller [5,6]. In practice, the measurement of surface roughness is also a complex process due to the wood's own properties and processing conditions [7].

The surface roughness of wood is influenced by its own properties and processing methods [7,8], and milling is one of the most important ways of processing wood. Kilic M et al. investigated the effect of various processing techniques on the surface roughness of beech and aspen, and the results showed that the surface roughness of beech and aspen wood differed under different processing methods [9]. Later, Malkoçoğlu A et al. analyzed the effect of feed speed and front angle on the surface quality of these five kinds of wood during planing with Oriental beech, Anatolian chestnut, Black alder, Scots pine, and Oriental spruce grown in Turkey, and the surface roughness of Oriental spruce was the best when the process parameters were consistent [10]. Aslan S et al. analyzed the surface roughness in the wood-cutting process and studied the effect of cutting direction, number

of inserts, and abrasive size on the surface roughness of golden cow shirt wood. The experimental results showed that a smoother surface can be obtained by radial cutting in golden cow shirt wood [11]; after that, Kamboj G et al. studied the optimum chip parameters for wood surface roughness of thermally modified (TM) wood at different process parameters and temperatures. The results showed that the surface quality of wood after TM is better than that of normal wood [12].

A study by Tomak E D et al. also found that TM can improve the surface roughness of weathered wood [13]. Many scholars have studied the surface roughness of wood because better surface quality can reduce the time and number of profiling [14], and a smooth wood surface is less susceptible to airborne impurities, moisture, and fungi, and is more suitable for painting and coating treatments to make it safe from weathering, etc. [15,16]. The simplicity and speed of measurement are also sought after to obtain the best possible surface quality of the wood. Traditionally, surface roughness is generally measured using a profilometer. Ozdemir T et al. used the stylus method to measure the surface roughness of pine wood for the analysis of the effect of chemical treatment on its surface quality [17]. Gündüz G et al. used the stylus method to measure the roughness of the faces of pine wood perpendicular to the fiber direction after TM [18]. Hiziroglu S et al. used the stylus profilometer to measure the surface roughness of pine wood used to analyze its effect on bond strength [19]. Later researchers resorted to other methods to predict the surface roughness of wood. CS et al. developed a laser imaging system to predict wood surface roughness using a two-dimensional Gaussian function model [20], after which Yuan D et al. designed a laser sensor system for online measurement of wood surface roughness [21], and Baradit E et al. worked out an optical interferometry of wood surface roughness with good correlation between the obtained surface roughness values and those obtained by a mechanical roughness meter [22].

It is not difficult to find in the above-mentioned scholars' studies that surface roughness and its measurement have a very important place in wood processing, and most of the wood processing experiments in the scholars' studies were performed on low and medium-speed equipment.

Based on the above, the paper will study the surface roughness of wood by high-speed machining center, and the main research contents are: milling the test object in the high-speed machining center, establishing the response surface model of process parameters and surface roughness by CCD experiment, fitting the parameter equation by ANOVA, and analyzing the change law of surface roughness. In addition, a method to predict surface roughness by chip size using an artificial neural network (ANN) model is proposed in the paper.

## 2. Materials and Methods

### 2.1. Materials

The experiment object was a dry pine block of 50 × 50 × 15 mm, and its material properties when it is smooth-grained are given in Table 1.

**Table 1.** Pine smooth grain material properties.

Density (kg/m <sup>3</sup> )	Compressive Strength (MPa)	Bending Strength (MPa)	Tensile Strength (MPa)	Shear Strength (MPa)	Modulus of Elasticity (MPa)	Poisson's Ratio	Coefficient of Friction	Water Content
420	50	87	104	10	12,000	0.65	0.35	8%

The type of milling cutter used was a 45° mortise and tenon cutter (Tenon Cutter, Yueqing Fuxin Hardware Tools Co., Ltd., Dongguan, China), and its processing thickness range was 10–17 mm. Dongguan, China), whose spindle speed range is 0–12,000 r/min and the feed speed range is 0–40 mm/s. Figure 1 shows the experiment material and machine tool, Figure 1a shows the experiment material, and Figure 1b shows the “Nanxing” MGK06 3-axis wood processing center.

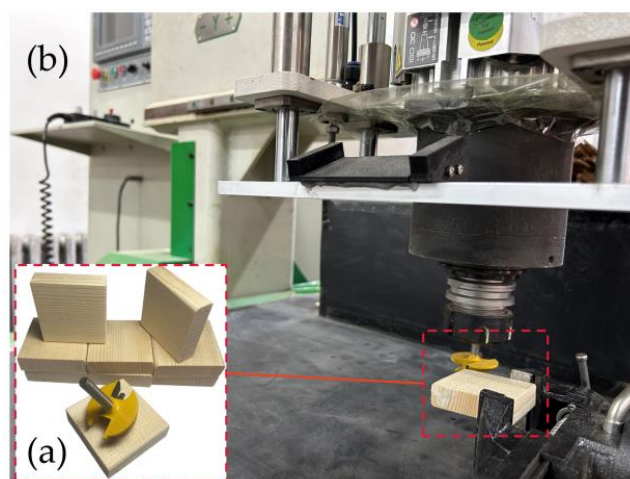


**Figure 1.** Material and machine tools. (a) Wood and knives; (b) Nanxing MGK06 3-Axis wood processing center.

## 2.2. Methods

### 2.2.1. CCD Experimental Analysis

CCD experiments are used to analyze the response of various factor indices and are widely used in design, formulation, and optimization [23]. The process parameters and groups of wood cutting were determined using the RSM design CCD experiment [24], and the literature [10,25–27] used spindle speed, feed speed, and depth of cut (or thickness) as influencing factors in the wood surface roughness study, and the spindle speeds were all low to medium. The wood processing machine tool used in this paper is a high-speed machining center; the experimental design will be spindle speed  $V_c$ , feed speed  $V_f$ , and depth of cut  $C_d$  as the influencing factors, the surface quality of wood as the evaluation index, the design of three factors and five levels of CCD experiment, Table 2 shows the experimental factors and levels.

**Table 2.** Response surface experimental level factors.

Level	Spindle Speed $V_c$ (r/min)	Factors Feeding Speed $V_f$ (m/min)	Cutting Depth $C_d$ (mm)
+1.68	11,000	1770	15
+1	10,000	1500	13
0	8500	1100	10
−1	7000	700	7
−1.68	6000	430	5

### 2.2.2. Surface Roughness and Chip Measurement

The measurement of wood surface roughness was performed using a digital display surface roughness measuring instrument (TIME3220, Beijing Times Raguang Technology Co., Ltd., Beijing, China) with a measurement range of 0–400  $\mu\text{m}$ , a sensor tip radius of 5  $\mu\text{m}$ , a resolution of 0.008  $\mu\text{m}$ , a sampling length of 0.8 mm each time, and a corresponding probe movement speed of 0.5 mm/s. The surface roughness of the experimental wood block with smooth grain was measured according to the standard for measuring the surface roughness of wood (GB-T12472-1990). The measurement area is illustrated by the group No. 1 experiment as an example, and a schematic diagram of the surface roughness measurement area is shown in Figure 2. Figure 2a shows the surface roughness measurement area, and each group of experiments contains four areas,  $m_1$ ,  $m_2$ ,  $m_3$ , and  $m_4$ , respectively, and the dimensional parameters of each area can be seen in the figure. The depth of cut is the variable in the CCD experiment, so the width of the measurement area in each group of experiments is a variable value. According to GB-T12472-1990, the

measurement of surface roughness should avoid wood knots, surface scratches, wood spurs, etc.; so the length of the measurement area in the text is divided longer (6 mm). The surface roughness of the wood is measured in Figure 2b, and the final surface roughness of each group of experiments is the average value of the four regions.

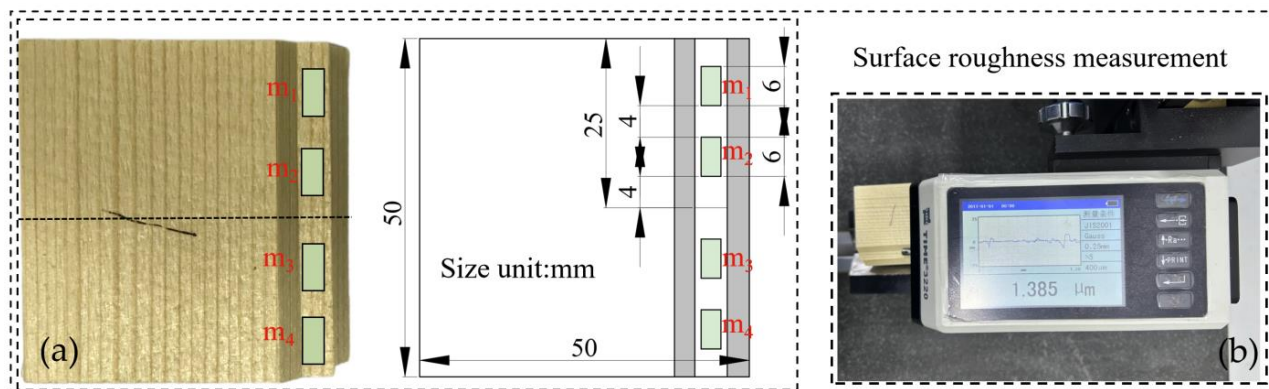


**Figure 2.** Wood surface roughness measurement. (a) Measurement area; (b) surface roughness paralleling measurement.

### 2.2.3. Wood Chip Size Measurement

In the paper, a portable optical microscope (KR-W04, Chengdu Kenrei Technology Co., Ltd., Chengdu, China) was used to measure the wood chip size, as shown in Figure 3, which shows the top view of the chip scattering distribution during wood cutting in the No. 24 group of experiments. From the experiment results, it can be obtained that in the whole scattering area, as the distance with the wood block gradually increases, the density of scattered wood chips first increases and then decreases, and the wood chips also gradually increase. The center of gravity position of the wood is used as the axis to establish the  $x$  and  $y$  coordinate system, and the chip size is measured in the experiment according to the divided area.  $L_a$  to  $L_d$  area in Figure 3a is four equally spaced areas, each area consists of three measurement areas, and the diameter of the contour circle of the measurement area is 20 mm, in which four measurement areas are on the  $y$ -axis equally spaced arc, and the remaining measurement areas are on the arc with the  $y$ -axis as the symmetry axis into  $\pm 15^\circ$  symmetry. Figure 3b shows the three measurement areas corresponding to each region, and the chips in the measurement areas were photographed by a 1000 times portable optical microscope to obtain the results. The average value of the chip size in the measurement areas in each region was taken as the result value of the chip size in one region for each group of experiments, and the total average value was solved for each group of experiments in addition to the average value of the chip size in the four regions.  $L_a$ ,  $L_b$ ,  $L_c$ , and  $L_d$  denote the average of chip sizes in the four selected areas, and  $L_A$  denotes the average of all chip sizes.

### 2.2.4. ANN Model Analysis Method

It is well known that chip size and surface roughness are affected by process parameters, and we have previously studied the effect of process parameters on chip size [28], and some scholars have successfully predicted the surface roughness of wood processing by establishing a wood surface roughness model under different process parameters through neural networks [25,29]. In this paper, surface roughness is predicted by chip size in the ANN model. The proposed ANN model is developed by using matlab neural network toolbox. The BP network is selected for prediction in the ANN model, and the BP network can learn and store a large number of input-output pattern mapping relationships without the need for known mathematical equations describing such mapping relationships. The flow chart of the ANN model prediction is shown in Figure 4. In Figure 4a, the BP network construction process is divided into three steps: BP network construction, BP network

training, and experiment result output. BP network construction selects the sample input and output, determines the topology and main functions, BP network training initializes the weight threshold of the network, calculates the fitting error according to the characteristics of the input samples, and finally outputs the fitted and predicted values. Figure 4b shows the BP network topology, which mainly consists of the input layer, hidden layer, and output layer, with input samples as  $L_a, L_b, L_c, L_d, L_A$ , and output samples as  $R_s$ .

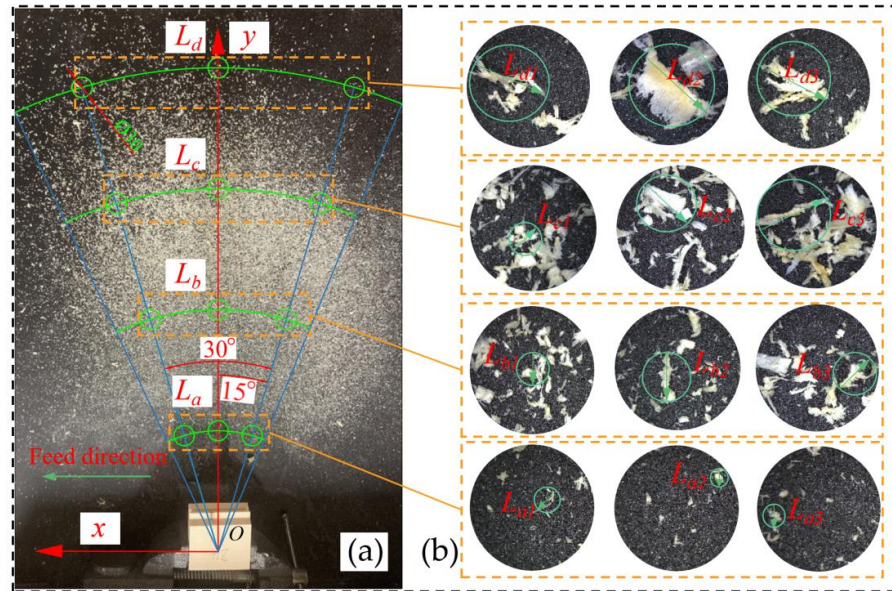


**Figure 3.** Top view of chip scattering area during wood cutting. (a) Four areas were selected at equal intervals for measuring chip size; (b) chip distribution state in the measurement zone.

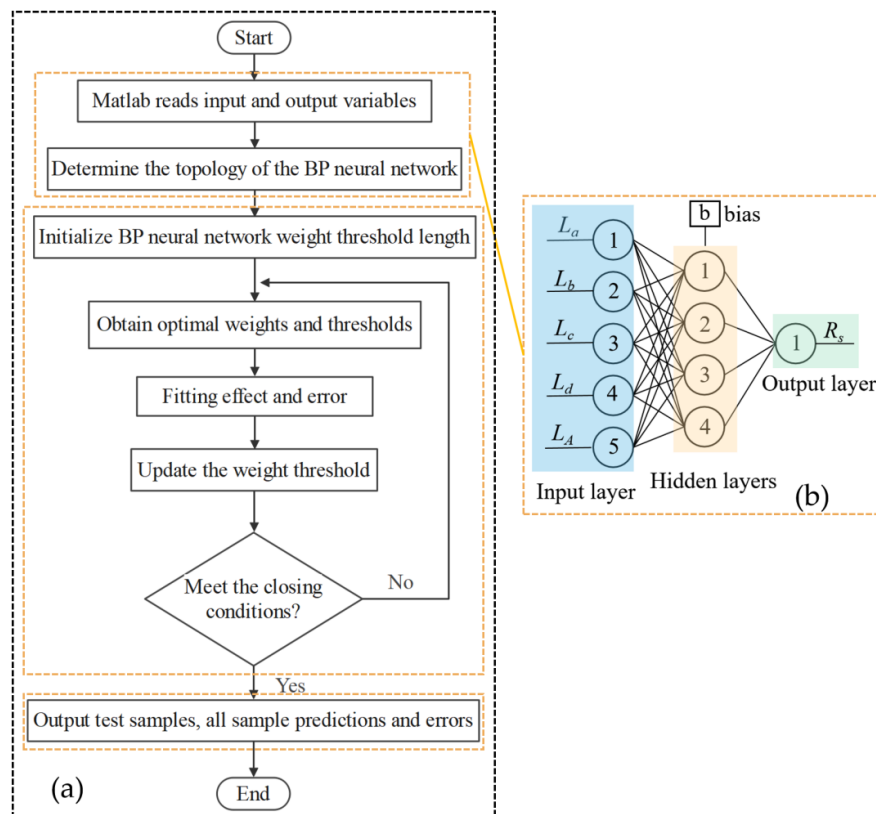


**Figure 4.** ANN model prediction process. (a) BP grid construction process; (b) BP network topology.

Considering that the relationship between surface roughness and chip size is difficult to express by mathematical equations, the ANN model can predict the relationship between chip size and surface roughness by training the available data. In the BP network, the hidden layer uses tansig as the activation function, purelin as the transfer function, trainlm as the training function, and the training method is gradient descent. The training number of samples is set to 1000, the learning rate is 0.1, the minimum error of the training target is 0.001, and the momentum factor is 0.01. In order to speed up the data convergence, the data need to be normalized before training, and the formula is calculated as in Equation (1) [29].

$$x' = \frac{x - x_{\min}}{x_{\max} - x_{\min}} \quad (1)$$

where:  $x'$  is the normalized value;  $x$  is the value of each group of the experiment;  $x_{\min}$  is the minimum value of the experiment;  $x_{\max}$  is the maximum value of the experiment.

The model fitting effect and error need to be analyzed and calculated in the BP network, and three analysis methods are used in this paper, which are experiment sample prediction effect analysis, fitting regression analysis, and model error analysis. Model error analysis contains mean square error (MSE), mean absolute percentage error (MAPE), and coefficient of determination  $R^2$ . These error analyses are used to assess the performance of the model [30,31] and can reflect the prediction error and the fitting effect of the model, and the model error is calculated as shown in Equation (2).

$$\begin{cases} \text{Error}(N) = y_i - y_o \\ \text{MSE} = \frac{1}{N} \sum_{i=1}^N \text{Error}(N)^2 \\ \text{MAPE} = \frac{1}{N} \sum_{i=1}^N \frac{\text{Error}(N)}{y_i} \end{cases} \quad (2)$$

where:  $N$  is the number of samples with a value of 26,  $y_i$  is the true value, and  $y_o$  is the predicted value.

### 3. Results and Discussion

#### 3.1. Experimental Analysis of Response Surfaces for Surface Quality

The wood milling experiment was conducted at the Forestry and Woodworking Machinery Engineering Technology Center of Northeastern Forestry University, at a temperature of 25 °C. The experiment results are shown in Table 3. In order to verify the prediction accuracy of surface roughness in the CCD experiment, six sets of supplementary verification experiments were added. In the table,  $V_c$  is the spindle speed (r/min),  $V_f$  is the tool feed speed (m/min),  $C_d$  is the depth of cut (mm), and  $R_s$  is the surface roughness of wood, which is lower for high-speed milling of wood compared with other wood processing equipment at low and medium speeds [25,32,33].

ANOVA and response surface model analysis were used to investigate the changing pattern of wood surface roughness during milling. The ANOVA for the surface roughness  $R_s$  is shown in Table 4, and the F-value of the total model in the table is 52.92, implying that the model is significant and there is only a 0.01% probability that the F-value is due to noise.  $p$ -values less than 0.0001 indicate that the model is highly significant, model terms A, B, C, AC,  $A^2$ ,  $B^2$ , and  $A^2C$  have  $p$ -values less than 0.05, and model terms are also highly significant, and the order of the degree of influence of single terms on surface roughness is  $A > B > C$ . The  $R^2$  of the model is 0.9686, the adjusted  $R^2$  is 0.9503, the predicted  $R^2$  is 0.9310, and the Adeq accuracy is 24.589, where the variability between the adjusted  $R^2$  and the predicted  $R^2$  is less than 0.2. They have consistent significance, and the Adeq accuracy can measure the ratio of signal to noise, and when the ratio is greater than 4, the accuracy of the model meets the design requirements, so the model accuracy is reliable.

The parametric equations of surface roughness and influencing factors are obtained from the above analysis and regression as shown in Equation (3):

$$R_s = 16.89 - 0.0039V_c + 0.11V_f - 1.64C_d + 0.004V_cC_d + 2.27 \times 10^{-7}V_c^2 - 0.0019V_f^2 - 2.59 \times 10^{-8}V_c^2C_d \quad (3)$$

**Table 3.** Experimental groups and results.

Group	$V_c$ Spindle Speed (r/min)	$V_f$ Feeding Speed (m/min)	$C_d$ Cutting Depth (mm)	$R_s$ Surface Roughness ( $\mu\text{m}$ )
1	8500	30.1134	10	1.854
2	8500	17.5	10	1.564
3	7000	25	13	2.415
4	10,000	25	7	1.421
5	5977.31	17.5	10	2.103
6	8500	17.5	10	1.654
7	10,000	10	7	0.833
8	10,000	25	13	1.159
9	7000	25	7	2.215
10	8500	4.88655	10	0.713
11	10,000	10	13	0.654
12	7000	10	13	1.586
13	7000	10	7	1.485
14	8500	17.5	10	1.881
15	8500	17.5	10	1.611
16	8500	17.5	10	1.459
17	8500	17.5	4.95462	1.313
18	8500	17.5	10	1.562
19	11,022.7	17.5	10	0.642
20	8500	17.5	15.0454	1.842
21*	10,000	17.5	10	2.029
22*	7000	17.5	13	1.086
23*	8500	25	13	2.612
24*	8500	10	10	1.075
25*	8500	10	7	1.102
26*	8500	17.5	7	1.263

The table with "\*" is a supplementary verification experiment.

**Table 4.** Surface roughness analysis of variance.

Model	Sum of Squares	Df	Mean Square	F-Value	p-Value	Significant
	4.67	7	0.6678	52.92	<0.0001	Yes
A-Spindle Speed	2.72	1	2.72	215.29	<0.0001	-
B-Feeding Speed	1.53	1	1.53	121.24	<0.0001	-
C-Cutting Depth	0.1399	1	0.1399	11.09	0.006	-
AC	0.0688	1	0.0688	5.45	0.0377	-
A <sup>2</sup>	0.0771	1	0.0771	6.11	0.0294	-
B <sup>2</sup>	0.1582	1	0.1582	12.54	0.0041	-
A <sup>2</sup> C	0.1012	1	0.1012	8.02	0.0151	-
Residual	0.1514	12	0.0126	-	-	-
Lack of Fit	0.0497	7	0.0071	0.3486	0.8989	no
Pure Error	0.1018	5	0.0204	-	-	-
Cor Total	4.83	19	-	-	-	-

"/ means no data.

The response surface model can visually reflect the influence law of the parameter changes of the interaction term on the surface roughness. Figure 5 shows the response surface model of the interaction term spindle speed  $V_c$  and cutting depth  $C_d$ . It can be concluded in Figure 5a,b that when the feed speed  $V_f$  is 17.5 m/min, the surface roughness of the wood gradually increases as the spindle speed  $V_c$  decreases and the depth of cut  $C_d$  increases, and the results are consistent with the conclusions reached by the authors of the literature [25,32]. On the contrary, if the spindle speed  $V_c$  increases and the depth of cut  $C_d$  decreases, the surface roughness of the wood gradually decreases.

In the ANOVA, the feed speed  $V_f$  is a highly significant factor, but the interaction term of the feed speed  $V_f$  and the interaction term of the squared term are insignificant terms, so for the feed speed  $V_f$  the effect of a single term on the surface roughness needs to be analyzed. As shown in Figure 6, when the spindle speed is 8500 r/min, and the depth of cut is 10 mm, the effect of feed speed on the surface roughness, the solid black line is the

roughness change curve. In Figure 6, it can be concluded that with the gradual increase of the feed speed, the surface roughness increases, and the surface quality of the wood becomes worse, which is in agreement with the results of N Škaljić's study [32]. The surface roughness is  $1.18 \mu\text{m}$  at a feed speed of  $10 \text{ m/min}$  at point A and  $1.849 \mu\text{m}$  at a feed speed of  $25 \text{ m/min}$  at point B. The increase in surface roughness is large when the feed speed is less than  $22 \text{ m/min}$ , and the increase in surface roughness is soothing when it is greater than  $22 \text{ m/min}$  because the main factor affecting the surface roughness at this time is not the feed speed  $V_f$ .

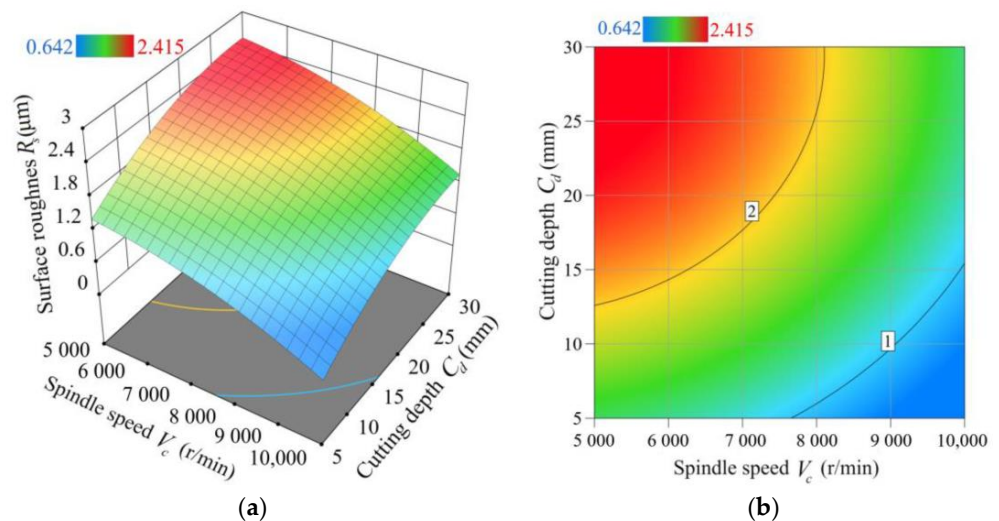


**Figure 5.** Graph of g-model of spindle speed  $V_c$  and depth of cut  $C_d$  at feed speed  $V_f$  of  $17.5 \text{ m/min}$  versus surface roughness  $R_s$ . (a) Surface model of surface roughness  $R_s$  versus spindle speed  $V_c$  and depth of cut  $C_d$  response; (b) response surface contour map.

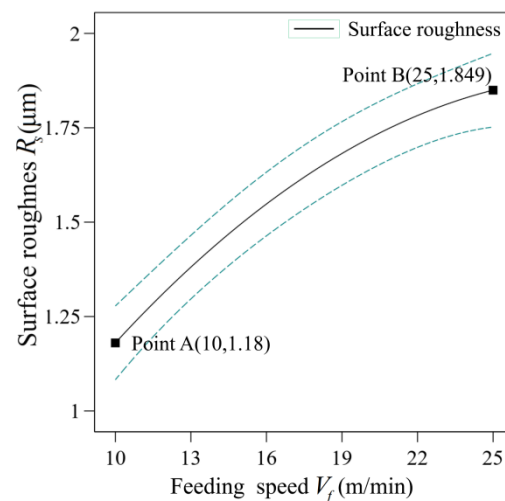


**Figure 6.** The effect of feed speed  $V_f$  on surface roughness when the spindle speed  $V_c$  and cutting depth  $C_d$  are  $8500 \text{ m/min}$  and  $10 \text{ mm}$ , respectively.

Minimizing the surface roughness of wood has always been sought after, and the optimal value of the surface roughness can be solved in the Design–Expert 13.0 optimization design module. The parameter ranges of spindle speed, feed speed, and depth of cut are  $7000\text{--}10,000 \text{ r/min}$ ,  $10\text{--}25 \text{ m/min}$ , and  $7\text{--}13 \text{ mm}$ , respectively. When the spindle speed is  $9965 \text{ r/min}$ , the feed speed is  $10.5 \text{ m/min}$ , and the depth of cut is  $11.8 \text{ mm}$ , the minimum value of surface roughness is  $0.649 \mu\text{m}$ .

### 3.2. Neural Network Analysis of Surface Roughness and Chip Size Correlation

The number of samples for the ANN model was 26 groups, which was consistent with the CCD experiment. Twenty-one of these data sets were used as training samples (80.77%), and five sets were used as experiment samples (19.23%). Table 5 shows the twenty-six sets of ANN model input and output samples, and each input sample contains five types of data.

**Table 5.** Chip sizes in selected areas.

Group	$L_a$ (mm)	$L_b$ (mm)	$L_c$ (mm)	$L_d$ (mm)	$L_A$ (mm)	Surface Roughness $R_s$ ( $\mu\text{m}$ )
1	0.382	0.692	1.131	1.821	1.007	1.854
2	0.284	0.541	0.871	1.376	0.768	1.564
3	0.492	0.759	1.820	1.988	1.265	2.415
4	0.319	0.462	0.948	1.310	0.760	1.421
5	0.427	0.557	0.955	1.241	0.795	2.103
6	0.306	0.549	0.888	1.455	0.800	1.654
7	0.215	0.313	0.823	1.414	0.691	0.833
8	0.301	0.439	1.793	2.528	1.265	1.159
9	0.421	0.663	1.158	2.470	1.178	2.215
10	0.245	0.388	0.942	1.445	0.755	0.713
11	0.296	0.393	0.865	1.095	0.662	0.654
12	0.464	0.671	1.347	2.354	1.209	1.586
13	0.369	0.489	0.775	1.630	0.816	1.385
14	0.423	0.668	0.889	3.110	1.273	1.881
15	0.391	0.505	0.918	1.903	0.929	1.611
16	0.324	0.484	0.914	1.417	0.785	1.459
17	0.309	0.477	0.911	1.445	0.786	1.313
18	0.312	0.514	0.727	1.368	0.730	1.562
19	0.283	0.405	0.944	1.447	0.770	0.642
20	0.414	0.687	1.475	1.909	1.121	1.842
21	0.504	0.695	0.769	1.345	0.828	2.029
22	0.321	0.518	1.018	1.964	0.955	1.086
23	0.514	0.834	1.241	2.140	1.182	2.612
24	0.315	0.439	0.725	1.314	0.698	1.075
25	0.301	0.438	1.127	2.275	1.035	1.102
26	0.326	0.494	0.809	1.391	0.755	1.263

Figure 7 gives the true and predicted values and errors of the five groups of experiment samples derived from the training samples of the BP network. The lines in the figure give the error between the true and predicted values, and the sample predicted values are the results obtained after 12 training sessions. The error in the graph is below 10% for other experiment samples except for the fifth experiment sample, which has a large error between the actual and predicted values. Considering the limitations of the chip measurement area, there will be a large error in the measurement of some chip sizes, which will lead to an increase in the chance error of the true value of some samples and a worse prediction, but the average error of all experimented samples is 5.62%, and the smaller average error indicates a better reliability of the predicted data [25], and the ANN model can be used to make a simple prediction of surface roughness by chip size.

Regression analysis of true and predicted values are usually used to assess the validity and accuracy of ANN models, and it has been pointed out in the literature [33] that the higher the correlation coefficient  $R$  is close to 1, the higher the accuracy of the model fit. The fitting results of the true and predicted values are shown in Figure 8; the fitted straight line in the figure can reflect the degree of fit of the sample. Figure 8a shows the fitting effect of 21 groups of training samples with a correlation coefficient  $R$  of 0.922, and Figure 8b shows the fitting effect of all samples trained with a correlation coefficient  $R$  of 0.92752. The fitting coefficients of the training samples and all samples can indicate the high prediction accuracy of the developed ANN model.

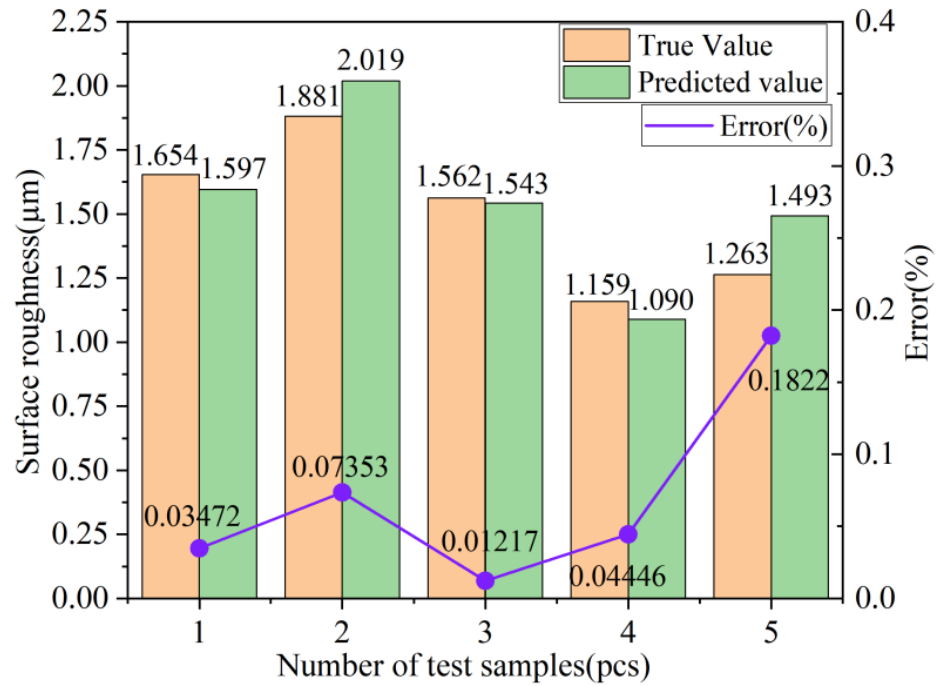


Figure 7. True and predicted values for the five sets of test samples.

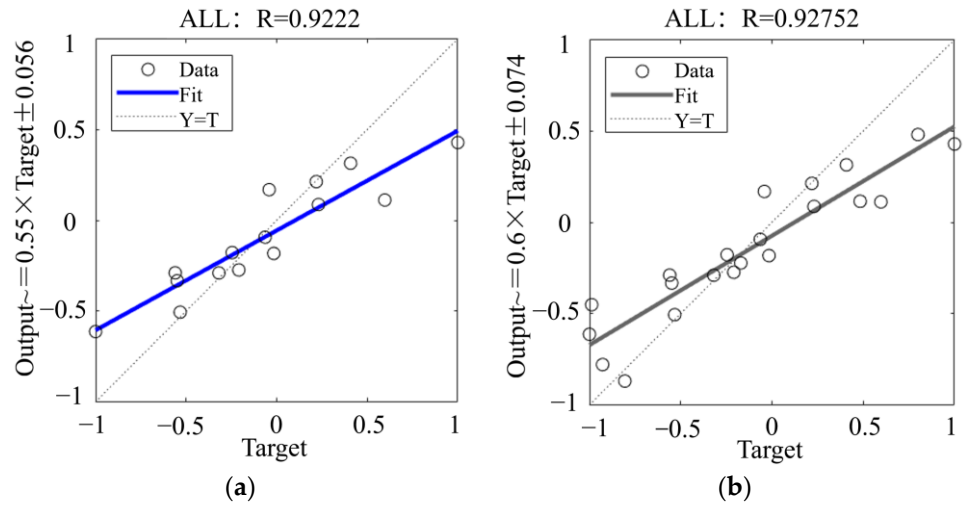


Figure 8. Fit of the true value to the predicted value. (a) Fitting effect of 21 sets of training samples; (b) fitted coefficients for all samples.

Figure 9 shows the predicted values of the ANN model for all samples compared to the true value results, using MSE, MAPE, and  $R^2$  to evaluate the performance of the ANN model. Demir A et al. pointed out that MAPE is one of the important evaluation criteria, and the performance of ANN models is high when its value is less than 0.1 [33], and Tiryaki S, in using MSE to evaluate the model, determined the performance of the network [25]. All samples in the paper had MSE values of 0.025, MAPE values of 0.01, and coefficient of determination  $R^2$  values of 0.95 in the predictions. These error levels are small, the ANN model has a small fitting error, and the ANN model can be used to predict the effect of chip size on surface roughness.

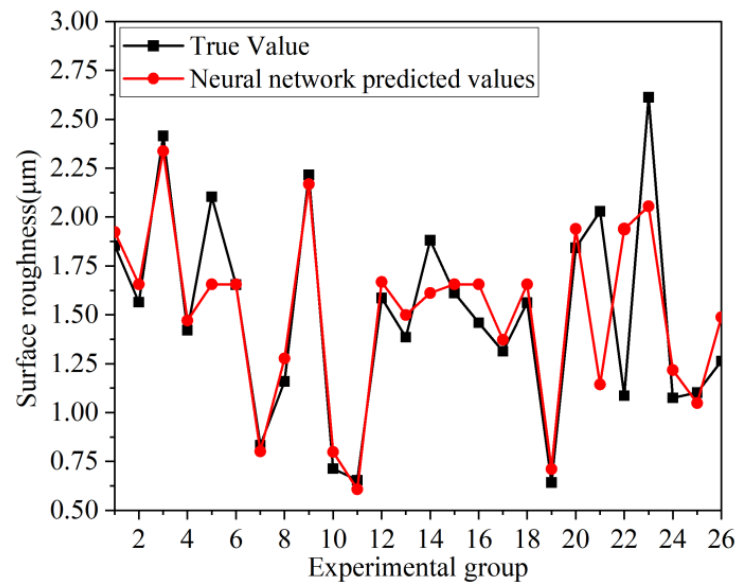


Figure 9. True and predicted values of all samples in the ANN model.

3.3. Surface Roughness and ANN Model Prediction Value Validation

The true values of 26 sets of trials with ANN model predictions and response surface predictions and errors are given in Figure 10. The figure shows that the error of the predicted values of groups 21 and 22 in the response surface model is 43.6% and 78.5%, while groups 21 and 22 are supplementary experiments, it can be concluded that the prediction accuracy of the response surface for supplementary experiments is not high, but the average error of the predicted values of the response surface is 12.2%, which is a relatively good result. The maximum error in the ANN model prediction was 41.9%, and this condition was caused by the error in chip size measurement. The average error in the ANN model prediction was 7.8%, which was smaller than the average error in the response surface prediction. The figure also shows that overall, the line graph of the predicted values of the ANN model is closer to the real values, which again validates that the ANN model can be used to analyze the effect of chip size on surface roughness.

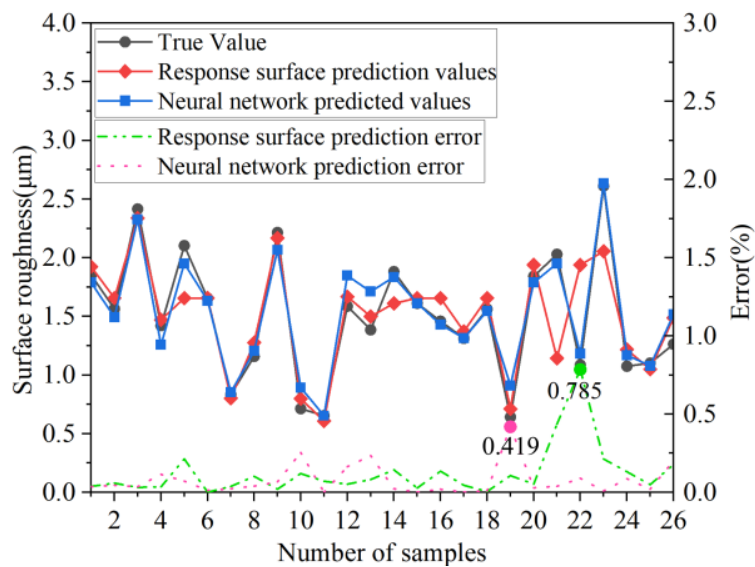


Figure 10. Twenty-six groups of surface roughness real value and predicted value fitting curve.

Table 6 shows the true values and response surface predictions and ANN model predictions and errors. The table shows the errors of each group of true values and predictions; in the overall prediction accuracy, the ANN model is higher than the response surface model predictions. As a result of this study, the chip size can be used to predict the surface roughness.

**Table 6.** Experimental true values with response surface predictions and neural network predictions and error results.

Group	True Value	Response Surface Predicted Values	Neural Network Predicted Values	Response Surface Prediction Error	Neural Network Prediction Error
1	1.854	1.924	1.789	0.038	0.035
2	1.564	1.656	1.493	0.059	0.045
3	2.415	2.337	2.328	0.032	0.036
4	1.421	1.471	1.257	0.035	0.115
5	2.103	1.656	1.952	0.213	0.072
6	1.654	1.656	1.634	0.001	0.012
7	0.833	0.802	0.853	0.038	0.023
8	1.159	1.277	1.205	0.102	0.040
9	2.215	2.168	2.067	0.021	0.067
10	0.713	0.798	0.894	0.120	0.254
11	0.654	0.608	0.653	0.071	0.001
12	1.586	1.668	1.848	0.052	0.164
13	1.385	1.499	1.711	0.082	0.235
14	1.881	1.611	1.836	0.144	0.023
15	1.611	1.656	1.612	0.028	0.001
16	1.459	1.656	1.430	0.135	0.020
17	1.313	1.372	1.315	0.045	0.002
18	1.562	1.656	1.546	0.006	0.010
19	0.642	0.711	0.911	0.107	0.419
20	1.842	1.939	1.788	0.053	0.029
21 *	2.029	1.144	1.951	0.436	0.038
22 *	1.086	1.938	1.184	0.785	0.089
23 *	2.612	2.055	2.635	0.213	0.009
24 *	1.075	1.217	1.169	0.132	0.087
25 *	1.102	1.048	1.079	0.049	0.021
26 *	1.263	1.487	1.517	0.178	0.200

The ‘\*’ in the table indicates supplementary experiments.

#### 4. Conclusions

In this study, the CCD experiment and ANN model were used to analyze the variation pattern of surface roughness of pine wood under various high-speed milling parameters. The response surface model in the CCD experiment responded to the influence of the influencing factors on the indexes, and the parameter equations fitted by ANOVA were a good fit for the experiment group and an average fit for the supplementary experiments. In addition, the surface roughness predicted by chip size in the ANN model analysis is more accurate than that of the response surface model in the CCD experiment. Therefore, the ANN model can be used to predict the surface roughness, but these two methods have a large error in the prediction of individual samples, and other experimental methods can be used in subsequent studies, especially increasing the groups of experiments in the ANN model can play an important role in reducing the error in the prediction of individual samples.

**Author Contributions:** Conceptualization, C.Y.; methodology, Y.M.; software, Y.M.; validation, T.L.; formal analysis, Y.M.; investigation, Y.D.; resources, W.Q.; data curation, Y.M.; writing—original draft preparation, Y.M.; writing—review and editing, Y.M.; visualization, C.Y.; supervision, Y.M.; project administration, Y.D.; funding acquisition, C.Y. and W.Q. All authors have read and agreed to the published version of the manuscript.

**Funding:** This research was funded by Heilongjiang Province Key R&D Project “Key Technology Research on 5G-based Digital Collaborative Processing Center for Passive Green Building Doors and Windows (2022ZX01A17)”.

**Data Availability Statement:** Not applicable.

**Acknowledgments:** We are very grateful to Ma Yan for his patient guidance and support in experimental and technical aspects.

**Conflicts of Interest:** The authors declare no conflict of interest.

## References

1. Chuttur, M.; Gillela, S.; Yadav, S.M.; Wibowo, E.S.; Sihag, K.; Rangppa, S.M.; Bhuyar, P.; Siengchin, S.; Antov, P.; Kristak, L.; et al. A comprehensive review of the synthesis strategies, properties, and applications of transparent wood as a renewable and sustainable resource. *Sci. Total Environ.* **2023**, *864*, 161067. [\[CrossRef\]](#)
2. Beims, R.F.; Rizkalla, A.; Kermanshahi-Pour, A.; Xu, C.C. Reengineering wood into a high-strength, and lightweight bio-composite material for structural applications. *Chem. Eng. J.* **2023**, *454*, 139896. [\[CrossRef\]](#)
3. Luo, B.; Zhang, J.; Bao, X.; Liu, H.; Li, L. The effect of granularity on surface roughness and contact angle in wood sanding process. *Measurement* **2020**, *165*, 108133. [\[CrossRef\]](#)
4. Aras, U.; Kalaycıoğlu, H.; Yel, H.; Durmaz, S. Fire performance, decay resistance and surface roughness of particleboards made from stone pine (*Pinus pinea* L.) cones. *Mugla J. Sci. Technol.* **2016**, *2*, 96–99. [\[CrossRef\]](#)
5. Aydin, I. Activation of wood surfaces for glue bonds by mechanical pre-treatment and its effects on some properties of veneer surfaces and plywood panels. *Appl. Surf. Sci.* **2004**, *233*, 268–274. [\[CrossRef\]](#)
6. Hiziroglu, S.; Zhong, Z.W.; Tan, H.L. Measurement of bonding strength of pine, kapur and meranti wood species as function of their surface quality. *Measurement* **2013**, *46*, 3198–3201. [\[CrossRef\]](#)
7. Gurleyen, L. The study for the strain of hardwood materials against machines and cutters in planning process. *Sci. Res. Essays* **2010**, *5*, 3903–3913.
8. Salca, E.A.; Hiziroglu, S. Evaluation of hardness and surface quality of different wood species as function of heat treatment. *Mater. Des.* **2014**, *62*, 416–423. [\[CrossRef\]](#)
9. Kilic, M.; Hiziroglu, S.; Burdurlu, E. Effect of machining on surface roughness of wood. *Build. Environ.* **2006**, *41*, 1074–1078. [\[CrossRef\]](#)
10. Malkoçoğlu, A. Machining properties and surface roughness of various wood species planed in different conditions. *Build. Environ.* **2007**, *42*, 2562–2567. [\[CrossRef\]](#)
11. Aslan, S.; Coşkun, H.; Kılıç, M. The effect of the cutting direction, number of blades and grain size of the abrasives on surface roughness of Taurus cedar (*Cedrus Libani* A. Rich.) woods. *Build. Environ.* **2008**, *43*, 696–701. [\[CrossRef\]](#)
12. Kamboj, G.; Gašparík, M.; Gaff, M.; Kačík, F.; Sethy, A.K.; Corleto, R.; Rezaei, F.; Ditommaso, G.; Sikora, A.; Kaplan, L.; et al. Surface quality and cutting power requirement after edge milling of thermally modified meranti (*Shorea* spp.) wood. *J. Build. Eng.* **2020**, *29*, 101213. [\[CrossRef\]](#)
13. Tomak, E.D.; Ustaomer, D.; Ermeýdan, M.A.; Yildiz, S. An investigation of surface properties of thermally modified wood during natural weathering for 48 months. *Measurement* **2018**, *127*, 187–197. [\[CrossRef\]](#)
14. Korkut, S. Performance of three thermally treated tropical wood species commonly used in Turkey. *Ind. Crops Prod.* **2012**, *36*, 355–362. [\[CrossRef\]](#)
15. Yildiz, S.; Yildiz, U.C.; Tomak, E.D. The effects of natural weathering on the properties of heat-treated alder wood. *BioResources* **2011**, *6*, 2504–2521.
16. Gašparík, M.; Gaff, M.; Kačík, F.; Sikora, A. Color and chemical changes in teak (*Tectona grandis* L. f.) and meranti (*Shorea* spp.) wood after thermal treatment. *Bioresources* **2019**, *14*, 2667–2683. [\[CrossRef\]](#)
17. Ozdemir, T.; Hiziroglu, S. Evaluation of surface quality and adhesion strength of treated solid wood. *J. Mater. Process. Technol.* **2007**, *186*, 311–314. [\[CrossRef\]](#)
18. Gündüz, G.; Korkut, S.; Korkut, D.S. The effects of heat treatment on physical and technological properties and surface roughness of Camiyani Black Pine (*Pinus nigra* Arn. subsp. *pallasiana* var. *pallasiana*) wood. *Bioresour. Technol.* **2008**, *99*, 2275–2280. [\[CrossRef\]](#) [\[PubMed\]](#)
19. Hernandez-Castaneda, J.C.; Sezer, H.K.; Li, L. Dual gas jet-assisted fibre laser blind cutting of dry pine wood by statistical modelling. *Int. J. Adv. Manuf. Technol.* **2010**, *50*, 195–206. [\[CrossRef\]](#)
20. Hu, C.; Afzal, M.T. Automatic measurement of wood surface roughness by laser imaging. Part I: Development of laser imaging system. *For. Prod. J.* **2005**, *55*, 158–163.
21. Yuan, D.; Han, Y. Computer-based Online Monitoring of wood surface roughness by Laser measurement. *J. Northeast For. Univ.* **2010**, *38*, 126–127.
22. Baradit, E.; Gatica, C.; Yáñez, M.; Figueroa, J.C.; Guzmán, R.; Catalán, C. Surface roughness estimation of wood boards using speckle interferometry. *Opt. Lasers Eng.* **2020**, *128*, 106009. [\[CrossRef\]](#)
23. Mishra, H.P.; Jalan, A. Analysis of faults in rotor-bearing system using three-level full factorial design and response surface methodology. *Noise Vib. Worldw.* **2021**, *52*, 365–376. [\[CrossRef\]](#)
24. Kim, P.; Haber, H.L.; Lloyd, J.; Kim, J.-W.; Abdoulmoumine, N.; Labbé, N. Optimization of thermal desorption conditions for recovering wood preservative from used railroad ties through response surface methodology. *J. Clean. Prod.* **2018**, *201*, 802–811. [\[CrossRef\]](#)

25. Tiryaki, S.; Malkoçoğlu, A.; Özşahin, Ş. Using artificial neural networks for modeling surface roughness of wood in machining process. *Constr. Build. Mater.* **2014**, *66*, 329–335. [[CrossRef](#)]
26. Meng, Y.; Wei, J.; Wei, J.; Chen, H.; Cui, Y. An ANSYS/LS-DYNA simulation and experimental study of circular saw blade cutting system of mulberry cutting machine. *Comput. Electron. Agric.* **2019**, *157*, 38–48. [[CrossRef](#)]
27. Novák, V.; Rousek, M.; Kopecký, Z. Assessment of wood surface quality obtained during high speed milling by use of non-contact method. *Drv. Ind.* **2011**, *62*, 105–113. [[CrossRef](#)]
28. Yang, C.; Liu, T.; Ma, Y.; Qu, W.; Ding, Y.; Zhang, T.; Song, W. Study of the Movement of Chips during Pine Wood Milling. *Forests* **2023**, *14*, 849. [[CrossRef](#)]
29. Bao, X.; Ying, J.; Cheng, F.; Zhang, J.; Luo, B.; Li, L.; Liu, H. Research on neural network model of surface roughness in belt sanding process for *Pinus koraiensis*. *Measurement* **2018**, *115*, 11–18. [[CrossRef](#)]
30. Boga, C.; Koroglu, T. Proper estimation of surface roughness using hybrid intelligence based on artificial neural network and genetic algorithm. *J. Manuf. Process.* **2021**, *70*, 560–569. [[CrossRef](#)]
31. Rifai, A.P.; Aoyama, H.; Tho, N.H.; Dawal, S.Z.M.; Masrurah, N.A. Evaluation of turned and milled surfaces roughness using convolutional neural network. *Measurement* **2020**, *161*, 107860. [[CrossRef](#)]
32. Škaljić, N.; Beljo Lučić, R.; Čavlović, A.; Obućina, M. Effect of Feed Speed and Wood Species on Roughness of Machined Surface. *Drv. Ind.* **2009**, *60*, 229–234.
33. Demir, A.; Birinci, A.U.; Ozturk, H. Determination of the surface characteristics of medium density fibreboard processed with CNC machine and optimisation of CNC process parameters by using artificial neural network. *CIRP J. Manuf. Sci. Technol.* **2021**, *35*, 929–942. [[CrossRef](#)]

**Disclaimer/Publisher’s Note:** The statements, opinions and data contained in all publications are solely those of the individual author(s) and contributor(s) and not of MDPI and/or the editor(s). MDPI and/or the editor(s) disclaim responsibility for any injury to people or property resulting from any ideas, methods, instructions or products referred to in the content.